

Oscillatory Magnetic Anisotropy in One-Dimensional Atomic Wires

P. Gambardella,¹ A. Dallmeyer,² K. Maiti,^{2,*} M. C. Malagoli,² S. Rusponi,¹ P. Ohresser,^{3,†} W. Eberhardt,^{2,‡}
C. Carbone,^{2,4} and K. Kern^{1,5}

¹*Institut de Physique des Nanostructures, Ecole Polytechnique Fédérale de Lausanne, CH-1015 Lausanne, Switzerland*

²*Institut für Festkörperforschung, Forschungszentrum Jülich, D-52425 Jülich, Germany*

³*European Synchrotron Radiation Facility, BP 200, F-38043 Grenoble, France*

⁴*Istituto di Struttura della Materia, Consiglio Nazionale delle Ricerche, Area Science Park, I-34012 Trieste, Italy*

⁵*Max-Planck-Institut für Festkörperforschung, Heisenbergstr. 1, D-70569 Stuttgart, Germany*

(Received 7 February 2004; published 10 August 2004)

One-dimensional Co atomic wires grown on Pt(997) have been investigated by x-ray magnetic circular dichroism. Strong changes of the magnetic properties are observed as the system evolves from 1D- to 2D-like. The easy axis of magnetization, the magnetic anisotropy energy, and the coercive field oscillate as a function of the transverse width of the wires, in agreement with theoretical predictions for 1D metal systems.

DOI: 10.1103/PhysRevLett.93.077203

PACS numbers: 75.30.Gw, 75.30.Cr, 75.70.Ak, 75.75.+a

A fundamental problem in magnetism is to understand how the magnetocrystalline anisotropy is determined by the symmetry and species of a magnetic atom and its neighbors in a material [1,2]. Driven by intense efforts to fabricate artificial structures with tailored magnetic properties, experiments on magnetic thin films have shown that the magnetocrystalline anisotropy energy (MAE) in two-dimensional systems is generally enhanced compared to the bulk [1], and that both the MAE and the coercive field H_c depend on the overlayer-substrate combination, overlayer thickness [1,3–5], strain [6], and morphology [7–9]. It was Néel who first suggested [10] that the reduced symmetry at surfaces and interfaces gives rise to magnetic surface anisotropy. Likewise, unusual magnetic anisotropy is expected in 1D systems [11,12]. The pair-bonding model of Néel, however, provides only an intuitive explanation of the parallel or perpendicular orientation of the easy magnetization axis with respect to broken symmetry planes [7]. The strength and sign of the MAE, on the other hand, derive from the electronic band structure of the material. *Ab initio* calculations [13] predict such effects to be particularly significant in 1D metal chains, where changes in the symmetry and atomic coordination produce strong modifications of the band structure compared to 2D films [14].

The present Letter provides the first experimental investigation of magnetic anisotropy in 1D atomic wires with variable width, spanning the crossover from 1D to 2D. Using x-ray magnetic circular dichroism (XMCD) we show that the dimensionality of Co wires deposited on a nonmagnetic Pt substrate has a nontrivial influence on the easy magnetization direction, which oscillates in the plane perpendicular to the wire axis going from monatomic wires to a monolayer film. The MAE and H_c decrease sharply in the double wires, but, contrary to the trend expected for increasing coordination of the Co atoms [2], rise again in the triple wires before converging

to monolayer values. The observed oscillations of the easy axis and MAE agree qualitatively with tight-binding calculations for both freestanding and Pd-supported Co wires of up to three atoms wide [11,12], suggesting that unusual magnetic behavior results from dimensionality-related modifications of the electronic structure of the wires.

The experiments were performed at beam line ID12B of the European Synchrotron Radiation Facility in Grenoble. Co wires of variable width were obtained by epitaxial row-by-row growth on the vicinal Pt(997) surface [15,16]. Co was evaporated from a high purity (99.99%) rod in ultra high vacuum (1×10^{-10} mbar) on clean Pt(997) at $T = 260$ K. At this temperature, surface diffusion causes the Co atoms to self-assemble in an array of parallel 1D wires by decorating the steps of the Pt(997) substrate, situated 20.2 ± 1.5 Å apart. In the row-by-row growth regime, the width of the wires is proportional to the Co coverage, with monatomic wires corresponding to 0.13 ML (monolayers). The Co coverage was calibrated on Pt(111) against the onset of perpendicular remanence and the magnitude of H_c measured by XMCD compared with combined Kerr-scanning tunneling microscopy experiments, both quantities depending critically on the coverage [3]. This method was found to be in agreement with the yield of a quartz microbalance, but more precise. Despite the accuracy of the coverage calibration, however, we note that the wires have a finite width distribution that reaches a maximum (± 0.6 atomic rows) for 0.5 ML Co, owing to the asynchronism of row-by-row growth on unequally spaced Pt terraces [15]. XMCD spectra (not shown here, see, e.g. Refs. [16,17]) were recorded at the Co $L_{2,3}$ edges (770–820 eV) by measuring the total yield of the photoemitted electrons for parallel and antiparallel alignment of the applied magnetic field \mathbf{B} with the light helicity. The sample was rotated about its polar and azimuthal axes with respect to the incident light direc-

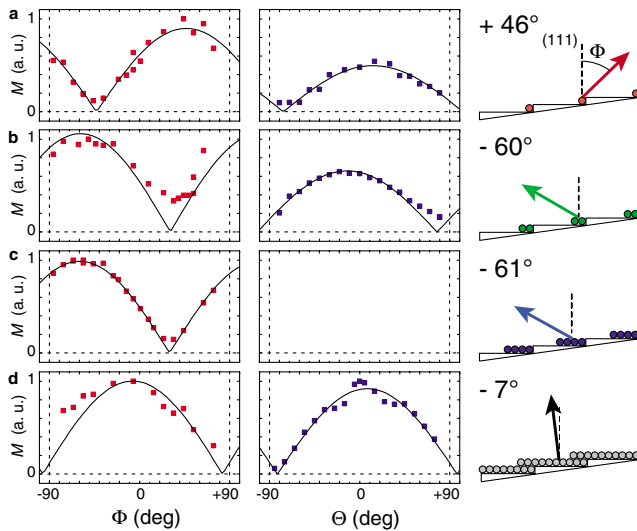


FIG. 1 (color online). Co wire magnetization M measured at a field B_r in the plane perpendicular to the wire axis (left column) and parallel to the wire axis and the (111) direction (right column). The data points represent the XMCD signal at the Co L_3 edge (779 eV) normalized by the total absorption yield. The solid lines evidence a $|\cos(x - x_0)|$ behavior with $x = \Phi, \Theta$, respectively, measured with respect to the (111) normal direction, as expected for uniaxial anisotropy. The diagrams show the easy axis direction as given by the maximum of the $|\cos|$ function. (a) 1-wires, $T = 10$ K, $B_r = 0.25$ T; (b) 2-wires, $T = 10$ K, $B_r = 1$ T; (c) 4-wires, $T = 10$ K, $B_r = 0.25$ T. No data were recorded in the plane parallel to the wires; (d) 1.3 ML, $T = 45$ K, $B_r = 1.5$ T.

tion in order to measure the XMCD (i.e., the magnetization projection) along different crystal orientations.

In Fig. 1 we report the Co wire magnetization M measured in the plane perpendicular (left hand side) and parallel (right hand side) to the wire axis at a field B_r , chosen so as to enhance the XMCD signal to 50% of saturation or above. Each time the sample was rotated, the magnetization was aligned in fields of up to 7 T and subsequently reduced to B_r . This procedure allowed us

to determine the easy axis of the wires, given by the direction where M is maximum. The $|\cos|$ behavior indicates a predominant uniaxial character of the magnetic anisotropy for the wires and monolayer samples. The easy direction is always found in the plane perpendicular to the n -wire axis, where n is the average width of the wires in atoms, whereas the hard direction is always parallel to the n -wire axis (parallel to the steps), in agreement with calculations of supported Co wires [11,12]. Owing to the lack of high symmetry directions [18], the magnetic anisotropy behavior in the plane perpendicular to the wire axis turns out to be of an extraordinary and complex character. The easy axis reverses from $\Phi = +46^\circ$ (step up direction) for the 1-wires to -60° (step down) for the 2-wires, as shown in Figs. 1(a) and 1(b). The reversal is abrupt and takes place between 0.17 and 0.19 ML, indicating that the magnetization of the entire system rotates at once. This rotation of the easy axis corresponds to a sign inversion of the MAE, an effect predicted by electronic structure calculations for both freestanding [11] and Pd-supported Co 1- and 2-wires [12] and attributed to changes in the relative filling of d orbitals with different symmetry [19]. Dipolar interactions are excluded as the cause for the magnetization rotation since (i) the in-plane dipolar field produced by the 2-wires is $B_{\text{dip}} < 0.1$ T $\ll B_r$, (ii) B_{dip} favors in-plane remanent magnetic order [5], which is not observed, and (iii) the magnetization rotates out-of-plane at higher coverage, indicating that the MAE overcomes dipolar interactions up to 1.3 ML and above. For $n = 3, 4$ the easy axis is found at $\Phi = -45^\circ, -61^\circ$, respectively; at 1.3 ML we observe a reorientation of the easy axis close to the (111) direction [Fig. 1(d)], which is consistent with the perpendicular magnetic anisotropy expected for monolayer Co films on Pt(111) [3].

As the wire transverse width increases, we find that the average MAE per Co atom, E_a , changes in a nonmonotonic way with n . Figure 2 reports the magnetization curves $M(\Phi_1)$ and $M(\Phi_2)$, where Φ_1 and Φ_2 represent two directions in the plane perpendicular to the wires ($\Theta = 0^\circ$) close to the easy and hard axis, respectively. A

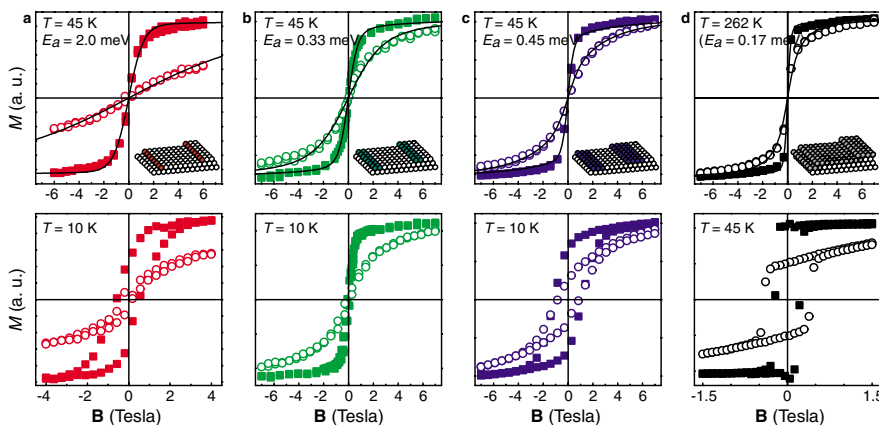


FIG. 2 (color online). Magnetization of (a) 1-wires, $\Phi_1 = +43^\circ$ (solid squares), $\Phi_2 = -57^\circ$ (open circles); (b) 2-wires, $\Phi_1 = -67^\circ$, $\Phi_2 = +23^\circ$; (c) 3-wires, $\Phi_1 = -7^\circ$, $\Phi_2 = +63^\circ$; (d) 1.3 ML, $\Phi_1 = -7^\circ$, $\Phi_2 = +63^\circ$. The data points represent the XMCD at the Co L_3 edge (779 eV) normalized by the L_3 absorption edge jump; solid lines are fits to the data (see text).

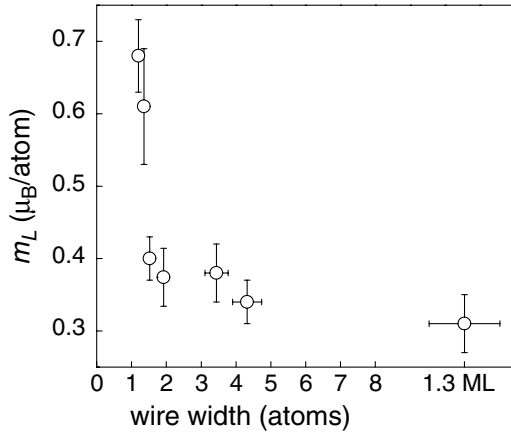


FIG. 3. Orbital magnetic moment m_L of Co wires as a function of width. m_L is obtained by applying the orbital XMCD sum rule to the spectra recorded at $T = 10$ K parallel to the easy axis direction, as explained in Ref. [17].

fit of $M(\Phi_1)$ and $M(\Phi_2)$ in the superparamagnetic regime (see below) shows that $E_a = 2.0 \pm 0.2$ meV/atom is largest for the 1-wires [17]. Since in small [2] as well as large [20] 2D clusters E_a is a rapidly decreasing function of the local coordination of the magnetic atoms, it is not surprising that E_a reduces abruptly to 0.33 ± 0.04 meV/atom in the 2-wires. The MAE reduction is such that the low-temperature hysteretic behavior almost vanishes going from the 1- to the 2-wires [Fig. 2(b)], despite the larger size of the superparamagnetic spin blocks in the 2-wires relative to the 1-wires. A strong decrease of the orbital magnetic moment also takes place between the 1- and the 2-wires (Fig. 3), precisely as the easy axis reverses from step up to step down. In the 3-wires, however, E_a shows a significant and unexpected 35% increment, up to 0.45 ± 0.06 meV/atom. In concomitance with the increased size of the spin blocks in the 3-wires, such increment favors again ferromagnetic order at $T = 10$ K [Fig. 2(c)]. This E_a upturn is opposite to that expected for the increasing average coordination of the Co atoms from 2- to 3-wires. Tight-binding calculations have revealed analogue E_a oscillations for freestanding 1D wires, suggesting that the observed effect is related to the specific electronic configuration of 1-, 2-, and 3-wires [11]. In our case, epitaxial strain, which results in fcc-hcp dislocations at 1 ML [15], is also liable to influence E_a , although it is unlikely a cause for the MAE oscillations.

Another unusual characteristic of the wires is the behavior of the coercive field H_c which shows strong oscillations with n (Fig. 4). In 2D systems, weak H_c oscillations with a 1 ML period have been observed during the growth of Co films on Cu(100) and attributed to minima in the step density and related MAE during layer-by-layer growth [9]. In 1D, such an effect could be mimicked by the varying density of kinks during row-by-row growth. However, the size of the effect is about 2 orders of

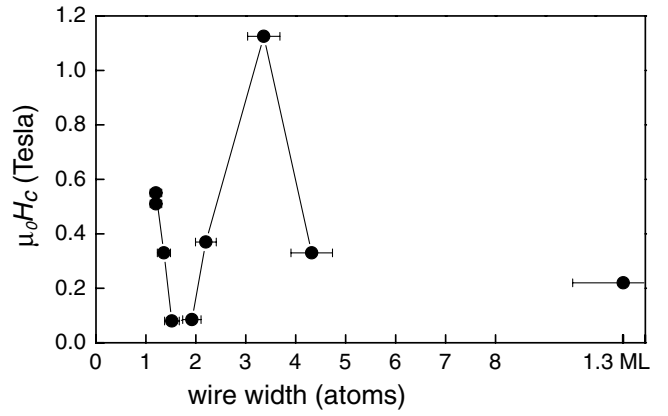


FIG. 4. $H_c(\Phi_1)$ measured at $T = 10$ K, except $T = 45$ K at 1.3 ML.

magnitude larger than observed for Co/Cu(100). Moreover, in the n -wires both H_c maxima and minima are observed for consecutive values of n , indicating that H_c depends on the transverse dimensions rather than on imperfections of the wire structure. Clearly, at fixed temperature, H_c reflects the MAE fluctuations, although the relation between H_c and E_a is also influenced by the temperature dependence of magnetic order and the competing mechanisms that determine the reversal of the magnetization in response to an external magnetic field. The crossover between $H_c(\Phi_1) > H_c(\Phi_2)$ to $H_c(\Phi_1) < H_c(\Phi_2)$ in Figs. 2(c) and 2(d) indicates that the dominant magnetization reversal mechanism changes from coherent rotation for the 1-, 2-, and 3-wires to reverse-domain nucleation [21] for the 1.3 ML film, where we observe $H_c(\Phi) \sim H_c(\Phi_1)/\cos(\Phi - \Phi_1)$.

The latter remark leads us to discuss the models used to obtain E_a from the data in Fig. 2. Assuming coherent reversal of the magnetization and uniaxial anisotropy for the 1-, 2-, and 3-wires, M was fitted in the superparamagnetic regime with a magnetic energy functional of the form [2]

$$E = -N\mathbf{m} \cdot \mathbf{B} - NE_a(\hat{\mathbf{m}} \cdot \hat{\mathbf{e}})^2, \quad (1)$$

where N is the average number of ferromagnetically coupled Co atoms in a spin block, \mathbf{m} is the magnetic moment per Co atom, and $\hat{\mathbf{e}}$ is the unit vector representing the easy axis direction. Here \mathbf{m} varies between 3.8 , 3.1 , and $3.1\mu_B$ for the 1-, 2-, and 3-wires, respectively, taking into account the decrease of the spin and orbital moment and the induced magnetization on the first and second nearest Pt neighbors [22]. By simultaneous, numerical integration of $M(\Phi_1)$ and $M(\Phi_2)$ over the Boltzmann distribution of energies (1), both E_a and N are obtained. The values of E_a derived in this way have been discussed above for $n = 1, 2, 3$. For the 1.3 ML film, the fit in Fig. 2(d) yields $E_a = 0.17 \pm 0.04$ meV/atom at $T = 262$ K ($\mathbf{m} = 2.9\mu_B$). However, the use of Eq. (1) in the

presence of domain nucleation cannot be justified. Independently of the magnetization reversal mechanism, E_a can be derived for a uniaxial system as [23]

$$E_a = \left[\int_0^{|\mathbf{m}|} BdM(\Phi_1) - \int_0^{|\mathbf{m}|} BdM(\Phi_2) \right] / \sin^2(\Phi_1 - \Phi_2), \quad (2)$$

provided that $M(\Phi_1)$ and $M(\Phi_2)$ reach saturation at the highest available field. Equation (2) yields $E_a = 0.15 \pm 0.02$ meV/atom for the 1.3 ML film at $T = 262$ K and 0.28 ± 0.07 , 0.51 ± 0.08 meV/atom for the 2- and 3-wires at $T = 45$ K, respectively, in agreement with the results obtained from Eq. (1).

Before concluding, we would like to discuss the results obtained by Eq. (1) for the 1-, 2-, and 3-wires relative to the spin block size N . It is known that in 1D the MAE is the key to observe long-range ferromagnetic order at finite temperature [17]. The latter is a metastable state whose lifetime at a given temperature depends on NE_a , as can be seen by comparing Figs. 2(a) and 2(b). In the superparamagnetic regime, however, the question arises as to what determines the extent of short-range ferromagnetic order (N in our case) as a function of the temperature and dimensions of the system [24]. For the 1-, 2-, and 3-wires at $T = 45$ K we obtain $N = 15$, 37, and 68, respectively, with about 10% uncertainty. These values are at odds with the expected exponential increase of the spin coherence length with n in finite 1D systems [25]. A likely explanation is that N is limited by defects in the wire structure that constitute weak magnetic links, such as, e.g., Pt atoms, fcc-hcp dislocations [15], Co vacancies, or nonmagnetic impurities. We cannot exclude, however, that spin fluctuations or nucleation of domain walls take place even in the n -wires [25,26], as the assumption of coherent magnetization reversal is strictly valid only if the spin blocks fluctuate faster than single spins, i.e., if NE_a is smaller than the exchange coupling energy of a Co spin summed over its neighbors ($\leq 2nJ$, with $J \approx 15$ meV in bulk hcp Co [27]).

In summary, reducing the dimensions of a magnetic layer down to 1D wires reveals a strikingly rich magnetic behavior as a function of the wire transverse width, which manifests itself in the observed fluctuations of the easy axis, MAE, and coercive field and in strong orbital magnetization.

We thank K. Larsson, S. S. Dhesi, and N. B. Brookes of beam line ID12B at the European Synchrotron Radiation Facility for help during the experiment and T. Cren for many stimulating discussions.

*Present address: Tata Institute of Fundamental Research, 400005 Mumbai, India.

[†]Present address: LURE, B.P. 34, F-91898 ORSAY, France.

[‡]Present address: BESSY G.m.b.H., D-12489 Berlin, Germany.

- [1] U. Gradmann, in *Handbook of Magnetic Materials*, Vol. 7, edited by K. H. J. Buschow (Elsevier, Amsterdam, 1993).
- [2] P. Gambardella *et al.*, *Science* **300**, 1130 (2003).
- [3] N. W. E. McGee *et al.*, *J. Appl. Phys.* **73**, 3418 (1993).
- [4] J. Shen *et al.*, *Phys. Rev. B* **56**, 11134 (1997).
- [5] J. Hauschild, U. Gradmann, and H. J. Elmers, *Appl. Phys. Lett.* **72**, 3211 (1998).
- [6] W. Wulfhekel *et al.*, *Europhys. Lett.* **49**, 651 (2000).
- [7] M. Albrecht *et al.*, *J. Magn. Magn. Mater.* **113**, 207 (1992).
- [8] W. Weber *et al.*, *Nature (London)* **374**, 788 (1995); R. K. Kawakami, E. J. Escorcia-Aparicio, and Z. Q. Qiu, *Phys. Rev. Lett.* **77**, 2570 (1996); S. S. Dhesi *et al.*, *ibid.* **87**, 067201 (2001); R. K. Kawakami *et al.*, *Phys. Rev. B* **58**, R5924 (1998); C. Boeglin *et al.*, *ibid.* **66**, 014439 (2002).
- [9] W. Weber *et al.*, *Phys. Rev. Lett.* **76**, 3424 (1996).
- [10] L. Néel, *J. Phys. Radium* **15**, 225 (1954).
- [11] J. Dorantes-Dávila and G. M. Pastor, *Phys. Rev. Lett.* **81**, 208 (1998).
- [12] R. Félix-Medina, J. Dorantes-Dávila, and G. M. Pastor, *New J. Phys.* **4**, 100 (2002).
- [13] B. Lazarovits, L. Szunyogh, and P. Weinberger, *Phys. Rev. B* **67**, 024415 (2003); **68**, 024433 (2003); J. Hong and R. Q. Wu, *ibid.* **67**, 020406 (2003); M. Komelj *et al.*, *ibid.* **66**, 140407 (2002); M. Eisenbach *et al.*, *ibid.* **65**, 144424 (2002).
- [14] A. Dallmeyer *et al.*, *Phys. Rev. B* **61**, R5133 (2000); R. Losio, K. N. Altman, and F. J. Himpsel, *Phys. Rev. Lett.* **85**, 808 (2000); C. Pampuch *et al.*, *ibid.* **85**, 2561 (2000); V. Rodrigues *et al.*, *ibid.* **91**, 096801 (2003).
- [15] P. Gambardella *et al.*, *Surf. Sci.* **449**, 93 (2000); *Phys. Rev. B* **61**, 2254 (2000).
- [16] P. Gambardella, *J. Phys. Condens. Matter* **15**, S2533 (2003).
- [17] P. Gambardella *et al.*, *Nature (London)* **416**, 301 (2002).
- [18] A. B. Schick, F. Máca, and P. M. Oppeneer, *Phys. Rev. B* **69**, 212410 (2004).
- [19] D. Wang, R. Wu, and A. J. Freeman, *Phys. Rev. B* **47**, 14932 (1993).
- [20] S. Rusponi *et al.*, *Nat. Mater.* **2**, 546 (2003).
- [21] D. V. Ratnam and W. R. Buessem, *J. Appl. Phys.* **43**, 1291 (1972).
- [22] S. Ferrer *et al.*, *Phys. Rev. B* **56**, 9848 (1998).
- [23] R. M. Bozorth, *Phys. Rev.* **50**, 1076 (1936).
- [24] J. C. Bonner and M. E. Fisher, *Phys. Rev.* **135**, A640 (1964).
- [25] E. V. Albano *et al.*, *Z. Phys. B Con. Mat.* **77**, 445 (1989); M. Pratzner *et al.*, *Phys. Rev. Lett.* **87**, 127201 (2001); *Phys. Rev. B* **67**, 094416 (2003).
- [26] O. Pietzsch *et al.*, *Science* **292**, 2053 (2001).
- [27] M. van Schilfgaarde and V. P. Antropov, *J. Appl. Phys.* **85**, 4827 (1999).